The Plant Journal (2007) **50**, 253–264 doi: 10.1111/j.1365-313X.2007.03046.x

Infection of tobacco with different *Pseudomonas syringae* pathovars leads to distinct morphotypes of programmed cell death

Magdalena Krzymowska[1], Dorota Konopka-Postupolska[1], Miroslaw Sobczak[2], Violetta Macioszek[1,†], Brian E. Ellis[3] and Jacek Hennig[1,*]

[1]*Institute of Biochemistry and Biophysics PAS, Pawinskiego 5a, 02-106 Warsaw, Poland,*

[2]*Department of Botany, Warsaw Agricultural University, Nowoursynowska 159, 02-776 Warsaw, Poland, and*

[3]*Michael Smith Laboratories, University of British Columbia, 2185 East Mall, Vancouver, BC V6T 1Z4, Canada*

Received 5 October 2006; revised 24 November 2006; accepted 11 December 2006.

[*]For correspondence (fax +48 22 658 4804; e-mail jacekh@ibb.waw.pl).

[†]Present address: Department of Biology, University of Lodz, Banacha 12/16, 90-237 Lodz, Poland.

Summary

Tobacco plants (*Nicotiana tabacum* cv. Xanthi-nc) infiltrated with either of two pathovars of *Pseudomonas syringae* – an avirulent strain of *P. syringae* pv. *tabaci* (Pst) or the non-host pathogen *P. syringae* pv. *maculicola* M2 (Psm) – developed a hypersensitive response (HR). There were considerable differences in HR phenotype, timing and sequence of cell dismantling between the two pathosystems. Following Psm infiltration, the first macroscopic signs were visible at 4.5 h post-infiltration (hpi). Simultaneously, increased plasma membrane permeability was observed, suggesting that the loss of cell membrane integrity initiates the macroscopic HR evoked by Psm. In contrast, after Pst treatment there was a distinct time lapse between the first signs of tissue collapse (9 hpi) and the occurrence of plasma membrane discontinuity (12 hpi). Ultrastructural studies of cells undergoing the HR triggered by Psm and Pst revealed distinct patterns of alterations in morphology of organelles. Moreover, while different forms of nuclear degeneration were observed in leaf zones infiltrated with Pst, we failed to detect any abnormalities in the nuclei of Psm-treated tissue. In addition, application of synthetic caspase inhibitors (Ac-DEVD-CHO, Ac-YVAD-CMK) abolished HR induced by Pst, but not Psm. Our observations suggest that different cell death mechanisms are executed in response to Psm and Pst. Interestingly, pre-inoculation with Pst, but not with Psm, induced a long-distance acquired resistance (LDAR) response, even though locally a typical set of defense responses, including acquired resistance, was activated locally in response to Psm. The failure of Psm to induce LDAR may be due to the rapid degeneration of bundle sheath cells resulting from Psm infection.

Keywords: hypersensitive response, non-host pathogen, avirulent pathogen, caspase inhibitors, acquired resistance.

Introduction

Pseudomonas syringae, a Gram-negative rod-shaped bacterium, is a versatile model for the study of plant pathogenesis (for review see Katagiri *et al.*, 2002). *Pseudomonas syringae* is subdivided into approximately 50 pathovars, based largely on the original host of isolation and pathogenicity, rather than biochemical or physiological criteria. Phylogenetic analyses indicate that strains of *P. syringae* can be divided into four major groups (Sarkar and Guttman, 2004) but, remarkably, strains assigned to the same pathovar are not always phylogenetically closely related (Sarkar and Guttman, 2004; Sawada *et al.*, 1999).

Non-host resistance is the most common form of plant disease resistance. This term describes the phenomenon when the entire plant species is resistant to a specific pathogen (Heath, 2000a). It is based on both pre-formed barriers and inducible active mechanisms. In the process of

evolution, non-host pathogens developed virulence factors that suppress or modulate plant defense responses, or help to optimize a hostile environment. This has enabled them to broaden their host range and to colonize new plants. As a counter-defense, plants have evolved mechanisms that enable them to sense and respond to modifications introduced by invaders into host cells, thus rendering the virulent pathogen avirulent.

It is often assumed that non-host and host avirulent pathogens evoke a similar multi-component resistance response. While initiation of the defense response requires perception by plants of the pathogen's presence (Nimchuk *et al.*, 2003), that recognition process appears to be based on different mechanisms, depending on whether or not the pathogen is able to colonize a given plant (Boller, 2005; Innes, 2004). Non-host defense responses are elicited by various microbe-derived structural components, referred to as pathogen-associated molecular patterns (PAMPs), which include lipopolysaccharides, flagellin and fragments of methylated bacterial DNA (for review see Nürnberger and Lipka, 2005). In contrast, during host interactions the plant surveillance system recognizes modification of host virulence targets and activates appropriate signalling cascades (van der Biezen and Jones, 1998).

The hypersensitive response (HR), an efficient defense strategy that restricts pathogen growth, can be activated during host as well as non-host interactions. The HR process involves programmed cell death (PCD) and manifests itself in tissue collapse at the site of pathogen attack (Heath, 1998). While caspases play a central role in the execution of cell death in animals, there are no evident homologues of caspases in plants; rather, metacaspases and vacuolar processing enzymes (VPEs) appear to regulate plant PCD (Hava-Nishimura *et al.*, 2005; Sanmartin *et al.*, 2005). The detailed mechanisms underlying plant PCD are still poorly elucidated. Apparently there are various forms of plant PCD (van Doorn and Woltering, 2005), and cells undergoing HR can also display distinct patterns of cellular changes depending on the experimental system (Christopher-Kozjan and Heath, 2003). The role of HR as a direct defense mechanism has been questioned (Heath, 2000b), but it is still broadly accepted that the HR is usually followed by enhanced resistance to secondary infection by the same, or even an unrelated, invader. In this manner, the HR serves as a signal of infection for the whole plant (Heath, 2000b).

In this study we compared the resistance responses of tobacco plants with two pathovars of *P. syringae*: a non-host pathogen, *P. syringae* pv. *maculicola*, and an avirulent strain of the host pathogen, *P. syringae* pv. *tabaci*. Both interactions result in an HR, although the response differs in the pattern of tissue necrotization and results in distinct cell-death morphotypes. In both systems the HR preceded the establishment of acquired resistance, although again, important differences were observed: Pst triggered a 'classical' form of acquired resistance expressed throughout the plant, whereas after Psm treatment, resistance induction was limited to pre-inoculated leaves.

Results

Patterns of tissue damage during HR induced by two pathovars of P. syringae

Plant defense responses against pathogens often involve restriction of the invader to its penetration site. When a high culture density of Psm (10^8 cfu ml^{-1}) was infiltrated into tobacco leaves, necrotic lesions developed. The first macroscopic symptoms were visible within 4.5 hpi (Figure 1a), and an ion-leakage assay showed that loss of cell membrane integrity was first detectable at that time (Figure 1e). Consistent with this, tissue from the infiltrated area began to stain with Evans blue (Figure 1c). On the other hand, inoculation with the same density of Pst elicited the first symptoms, visible as glazing of abaxial leaf surfaces, at 9 hpi, and Evans blue uptake and ion leakage were first detected at 12 hpi (Figure 1b,d).

Thus for Pst the necrotization process was significantly delayed and extended in comparison with Psm, and the macroscopic necrotization distinctly preceded plasma membrane permeabilization (Figure 1b,f). To characterize further HRs triggered by Psm and Pst, we checked the kinetics of *Hsr203J* and *Hin1* induction. *Hsr203J* expression has been shown to be strongly correlated with PCD induced in tobacco by various pathogens (Tronchet *et al.*, 2001). Similarly, *Hin1*, originally identified as a gene induced by harpin, is commonly used as a marker for HR in tobacco (Gopalan *et al.*, 1996). We found that both these HR markers were induced in the early stages of infection, 3 and 4.5 hpi after Psm and Pst inoculation, respectively, and their expression remained elevated by 6 hpi in both pathosystems (Figure 1g). However, it should be noted that expression of both *Hsr203J* and *Hin1* was much stronger in response to Pst.

Morphotypes of cell death triggered by host and non-host bacteria

The observed differences in the development of HR in response to Psm and Pst infection led us to examine other aspects of the PCD process. Transmission electron microscopy (TEM) revealed ultrastructural changes in the nuclei, chloroplasts and mitochondria in mesophyll cells from areas infiltrated with either bacterial strain. In Psm-inoculated tissue, chloroplasts in particular displayed major structural changes. Increased numbers of round plastids were observed as early as 1.5 hpi (Figure 2a, section A), in contrast to the usual crescent shape seen in non-infected leaves, and by 4.5 hpi they had completely disintegrated (Figure 2a, section B; Figure S1d in Supplementary Material). In contrast, at the

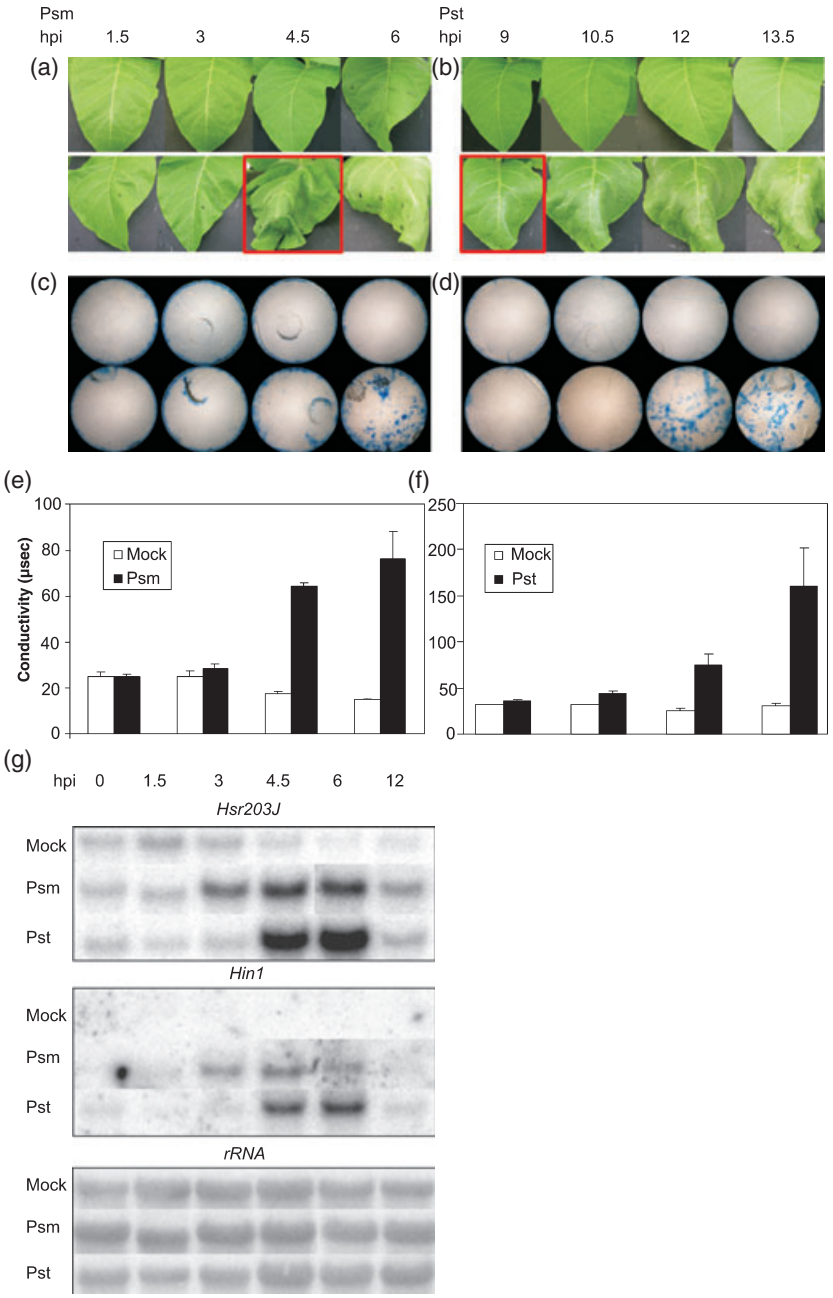

Figure 1. Differences in physiological and molecular markers of cell death in response to treatments with two *Pseudomonas syringae* pathovars.
(a, b) Pictures of leaves taken at various time points after Psm (a) or Pst infiltration (b). Leaves with the first visible symptoms of tissue necrotization are marked with red frames.
(c, d) At the same time points, membrane permeability was tested as Evans blue dye uptake after Psm (c) or Pst (d) treatment. (a–d) Upper lines represent mock-inoculated leaves.
(e, f) Cellular ion leakage to the apoplast was measured after floating eight leaf discs on the milliQ water surface.
(g) *Hsr203J* and *Hin1* transcript accumulation in response to Psm or Pst infection. *rRNA* hybridization shown as a loading control. All experiments were performed twice, with similar results.

same time no dramatic morphological changes were observed in the mitochondria (Figure 2a, sections A,B; Figure S1d,f). In the nuclei, the chromatin had already become more electron-translucent by 1.5 hpi (Figure 2a, section A), but the integrity of the nuclear envelope was retained up to the time of cell wall disruption (6 hpi, Figure S1h).

After Pst inoculation, the nucleoplasm became electron-translucent by 3 hpi and heterochromatin almost completely disappeared (Figure 2a, section C; Figure S1l). However, when the first macroscopic symptoms later became evident (9 hpi), osmiophilic heterochromatin-like material was seen to accumulate along the invaginated nuclear envelope, and nuclear blebbing was observed (Figure 2a, section D; Figure S1n). At this time point, some mitochondria in the Pst-challenged tissue had a reduced number of cristae, while the envelope of others began to disintegrate and chloroplasts began to change shape.

Changes in nuclear morphology were also analyzed by DAPI staining at the time of tissue collapse. We failed to detect any abnormalities in nuclei of Psm-inoculated tissue (Figure 2b, sections A–D) compared with the control

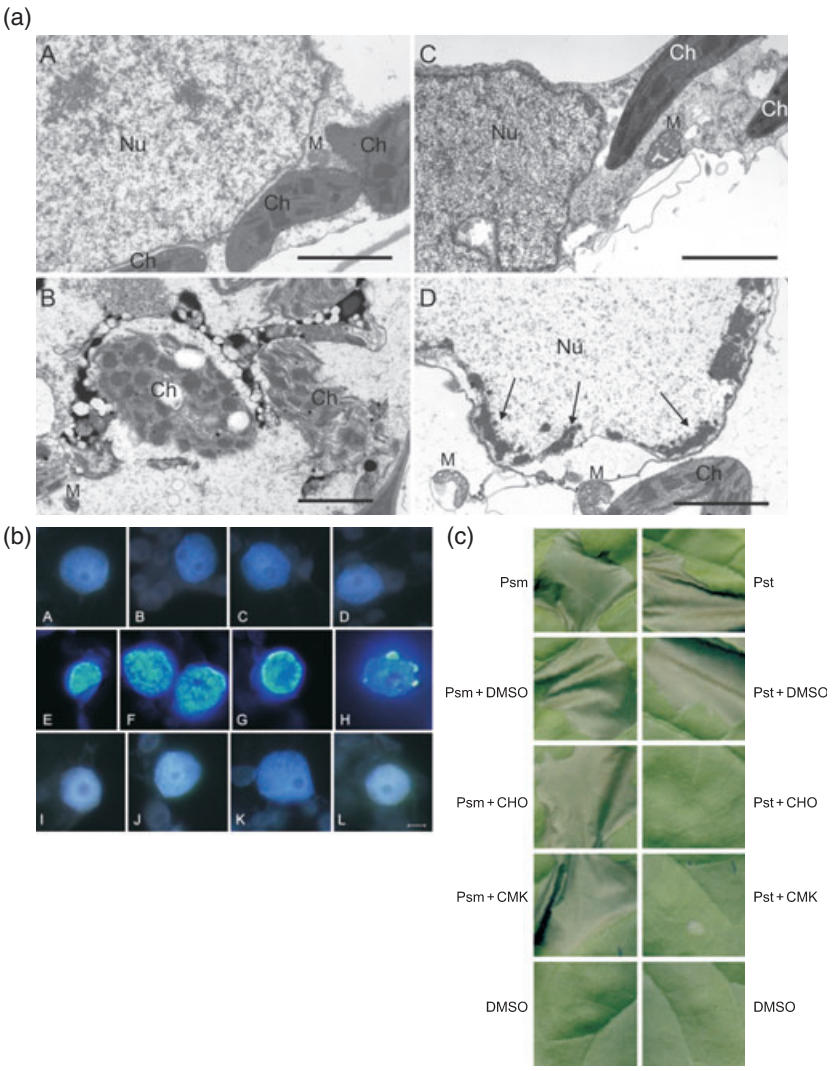

Figure 2. Ultrastructural and macroscopical features of cell death.
(a) Transmission electron micrographs showing changes in ultrastructure of organelles in response to infection with two pathovars of *P. syringae.* Samples were collected from zones infiltrated with Psm at 1.5 hpi (a) and 4.5 hpi (b), or Pst at 3 hpi (c) and 9 hpi (d). Arrows point to heterochromatin-like grains. Ch, chloroplast; M, mitochondrion; Nu, nucleus. Bars, 2 μm.
(b) Different stages of nucleus degeneration during the hypersensitive response (HR) to bacterial infection. DAPI staining to visualize nucleus morphology at the time of tissue collapse in the infiltration zones of leaves infected with bacteria. Images were analyzed by fluorescence microscopy. Bar, 2 μm. A–D, images from Psm-; E–H from Pst-; I–L from mock-inoculated leaves.
(c) Synthetic caspase-specific inhibitors abolish HR cell death induced by Pst but not by Psm. Tobacco leaves were infiltrated with either one of two pathovars of *P. syringae* (10^8 cfu ml^{-1}) in the presence or absence of caspase inhibitors. Ac-YVAD-CMK and Ac-DEVD-CHO were used at 200 μM each. Bacteria supplemented with DMSO (0.4%), or DMSO or bacteria alone, were infiltrated as controls. Inhibitors were added to suspensions of bacteria immediately before infiltration. Plants infected with bacteria were kept at 22°C as described in Experimental procedures. The pictures were taken at 48 hpi. All experiments were repeated twice, with similar results.

(Figure 2b, sections I–L). To account for the possibility of missing the proper time window, other time points from 6 to 24 hpi were also examined, but no changes in nucleus structure were observed (data not shown). In contrast, nuclei in Pst-challenged tissue (Figure 2b) displayed a range of structural abnormalities, including crescent-shaped nuclei (section E), granular chromatin (F), chromatin concentrated along the nuclear envelope (G) and nuclear blebbing (H). These features have frequently been considered characteristic of cells undergoing apoptotic cell death, but recently they have also been reported to occur during autophagy (van Doorn and Woltering, 2005).

Vacuolar processing enzyme (VPE) has been recently shown to be essential for vacuole-mediated cell death during the HR in tobacco and *Arabidopsis thaliana* (Hatsugai *et al.*, 2004; Rojo *et al.*, 2004). Although structurally unrelated to caspases, VPE possesses caspase-1 activity which can be blocked by a caspase-1 inhibitor and, to a lesser extent, by a caspase-3 inhibitor (Hatsugai *et al.*, 2004; Nakaune *et al.*, 2005; Rojo *et al.*, 2004). Strikingly, Psm-induced cell death was not abolished by application of synthetic inhibitors of mammalian caspase-1 and caspase-3 (Figure 2c), whereas both inhibitors suppressed cell death triggered in tobacco by challenge with the host avirulent strain, Pst. Taken together, these data suggest that the cell-death pathways operating in these two interactions differ significantly from each other.

Local defense responses are activated in tobacco plants by both Psm and Pst

Reactive oxygen species accumulation is a typical response of plant cells to pathogen challenge. When the nitroblue tetrazolium (NBT) assay was applied to monitor the level of superoxide anion in inoculated leaves, the level of O_2^- was found to increase by 3 and 9 hpi in Psm- and Pst-infected

leaves, respectively (Figure 3a,b), but this increase was much more pronounced (two- to threefold) in Pst-infected leaves. To characterize local defense responses further, infected leaves were harvested at various time points post-infiltration, and salicylic acid (SA) levels were analyzed by HPLC. As shown in Figure 3(c), the level of total SA (free SA and its conjugate) began to rise at 6 hpi in response to both bacterial strains, reaching approximately 0.6 and 1.0 μg g^{-1} FW by 24 hpi in Psm- and Pst-infiltrated tissue, respectively. This is a more rapid accumulation that that reported for the classical tobacco–TMV (tobacco mosaic virus) pathosystem, where salicylic acid began to rise at 24–36 hpi and reached the level of 1.0 μg g^{-1} FW by 72 hpi (Malamy *et al.*, 1990). As SA accumulation usually induces activation of *PR* genes,

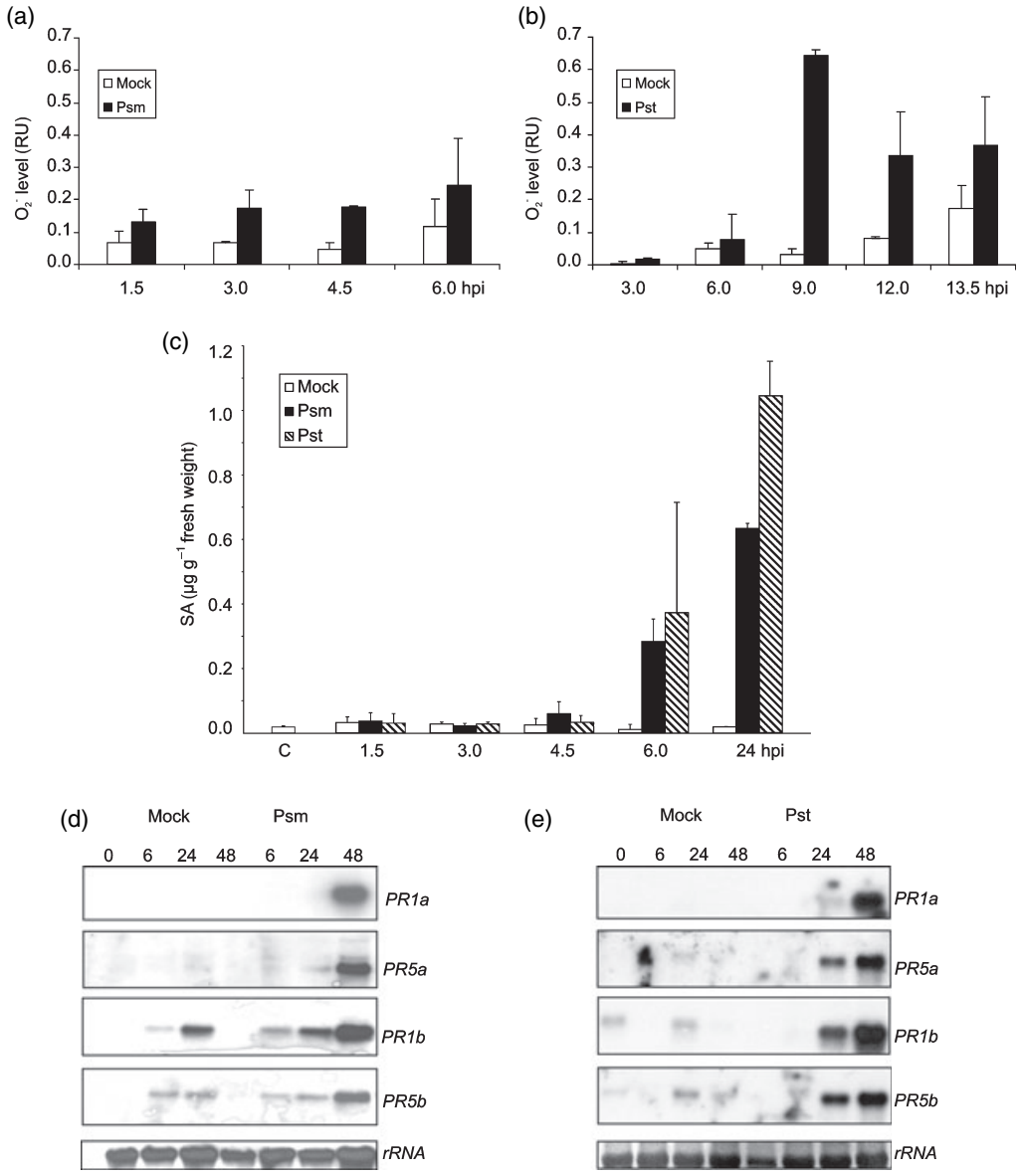

Figure 3. Activation of local defense responses after inoculations with bacteria.
(a, b) Generation of superoxide anion (O_2^-) was studied in eight leaf discs floated on reaction buffer containing nitroblue tetrazolium (NBT). Samples were collected every 1.5 h. Graphs show mean O_2^- content in duplicate samples, expressed in relative units (RU = A_{560}/6.3 cm^2). Error bars, SD. The experiment was performed three times, with similar results.
(c) Total SA levels in mock-, Psm- or Pst-inoculated leaves at different times after infection. Results are means of two samples. The experiments were performed twice, with similar results. Error bars, SD.
(d, e) Local expressions of genes coding for acidic and basic isoforms of PR-1 and PR-5 proteins. RNA was isolated at different time points post-infection from fully developed tobacco leaves. Each lane contained 10 μg total RNA. After hybridization with a probe specific for an acidic PR isoform, the probe was removed and the same membrane was rehybridized with a probe for the corresponding basic isoform. The amount of RNA on the blot was visualized by rehybridizaton with a probe for rRNA. The experiment was repeated twice.

expression of *PR-1* and *PR-5* genes in the infiltrated leaves was tested by Northern blotting at 6, 24 and 48 h after bacterial inoculation. As shown in Figure 3(d,e), acidic isoforms of pathogenesis-related proteins PR1 and PR5 were locally induced relative to mock-treated control plants. Increased transcript accumulation of basic isoforms was also detected in both mock- and bacteria-treated leaves, but expression was much stronger and more persistent in the latter. The induction of basic isoforms in mock-treated plants can probably be ascribed to tissue damage resulting from the experimental procedure.

Pathogen attack also induces rapid synthesis of callose in the challenged plants but, as shown in Figure S2, we found marked differences in callose deposition depending on the bacterial strain used for infiltration. At the time of tissue collapse, callose deposition was easily detectable in Pst-treated tissue (Figure S2h). The signal was distributed throughout the infiltrated zone. In contrast, the number of callose deposits elicited by Psm was very limited at either 4.5 hpi (Figure 2Se) or 6 hpi (data not shown). Necrotization of the tissue precluded longer-term experiments, but TEM analyses of corresponding sections revealed the presence of locally thick layers of callose confined to the Pst infection sites (Figure 2Si), whereas only thin, if any, layers were observed at Psm infection sites (Figure 2Sf).

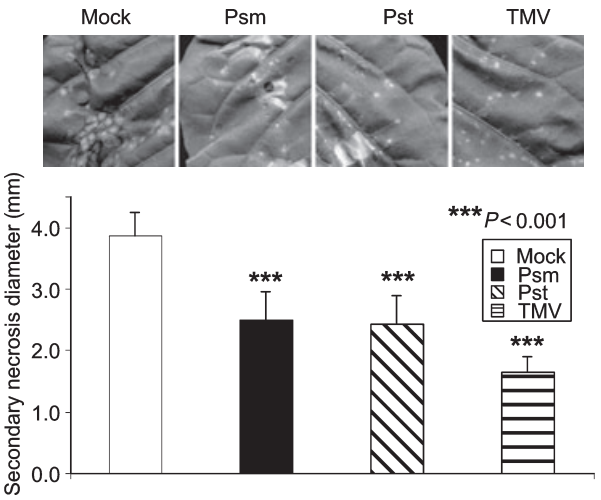

Figure 4. Quantification of short-distance acquired resistance against tobacco mosaic virus (TMV) after pre-inoculation with two strains of *Pseudomonas syringae*.
Uninfected areas of bacteria infiltrated leaves were challenged with TMV. Size of necrotic lesions was measured 7 days after secondary infection. Lesion size is the mean of 30 lesions on three plants SD. Plants pre-inoculated with TMV or water were used as controls. Asterisks indicate a significant difference between the treatment and the water control. The experiment was performed three times, with similar results.

Short-distance acquired resistance

In response to both pathovars, tobacco plants displayed local activation of a typical set of biochemical and molecular reactions, but with clear differences in timing and/or intensitiy. To assess the ability of these local reactions to induce increased resistance in non-infected regions of infiltrated leaves (short-distance acquired resistance, SDAR), we compared the diameters of TMV-induced necroses in leaves previously infected at neighbouring sites with Psm or Pst (10^8 cfu ml^{-1}). Mock- or TMV-pre-inoculated plants were used as negative and positive controls, respectively. Six days after primary inoculation, non-infected areas of these infected leaves were challenged with TMV, and the diameters of the resulting necroses (10 per leaf) were measured 7 days later. Reduction in the size of such secondary necroses is an indication of the induction of SDAR by the primary infection events. In all pathogen-pre-treated leaves, the secondary TMV-necrotic lesions were significantly smaller than in mock-pre-treated control leaves (Figure 4), including those treated with either bacterial pathovar.

Long-distance acquired resistance is not established in non-host interaction

An analogous approach was used to assess the effectiveness with which acquired resistance was induced systemically in parts of infected plants remote from the initial infection. Three leaves of tobacco plants were first either mock-inoculated or inoculated with one of the *P. syringae* pathovars. Seven days after this primary inoculation, upper non-inoculated leaves were challenged with TMV, and the size of the necrotic lesions formed after this TMV infection was measured 7 days later. As shown in Figure 5(a), the average lesion size differed markedly depending on the primary treatment. Psm inoculation resulted in no significant reduction in lesion size relative to mock-inoculated plants. In contrast, primary inoculation with Pst led to a significant decrease in TMV lesion size, reflecting the establishment of long-distance acquired resistance (LDAR). Consistent with this, we observed the accumulation of PR-1a, the molecular marker of LDAR, only in upper non-inoculated leaves of Pst-pre-treated plants (Figure 5b).

Time course of vascular tissue disorganization after bacterial infection

As the vascular tissue that interconnects distinct parts of a plant represents the most likely means of systemic communication, we analyzed the state of vascular bundles in bacteria-infiltrated leaves. As shown in Figure 6, we found dramatic differences in the kinetics of vascular tissue decay between leaves infiltrated with each of the two pathovars. In veins of leaves infected with the non-host pathogen, single cell-death events could be detected by 3 hpi (Figure 6a), and 1.5 h later most of the parenchymatous vascular bundle cells

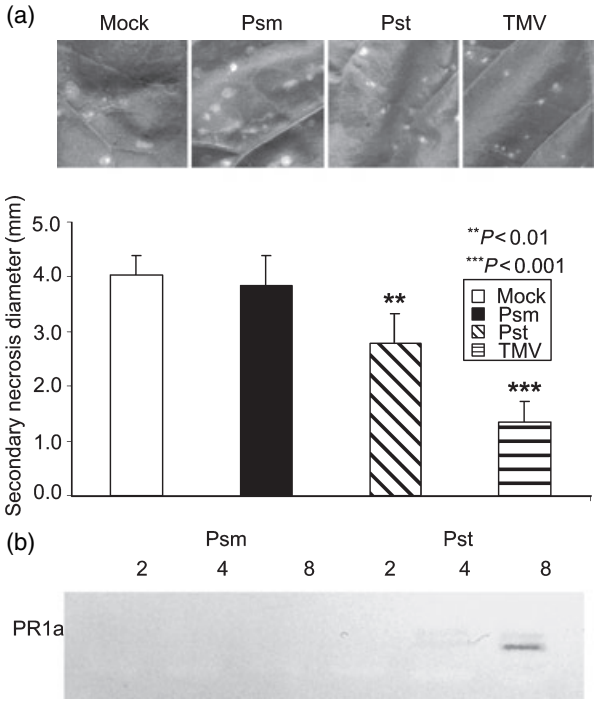

Figure 5. Long-distance acquired resistance induced after infection with *Pseudomonas syringae* pathovars.
(a) Quantification of long-distance acquired resistance against tobacco mosaic virus (TMV) after pre-inoculation with two strains of *Pseudomonas syringae*. Upper uninfected leaves of plants challenged with bacterial pathogens were inoculated with TMV. The diameters of necrotic lesions were measured 7 days after secondary infection. Lesion size is the mean of 30 lesions on three plants ±SD. Plants pre-inoculated with TMV or water were used as controls. Asterisks indicate a significant difference between the treatment and the water control. The experiment was performed three times, with similar results.
(b) The presence of PR-1a in upper non-inoculated leaves of Psm- or Pst-pretreated plants. Crude protein extracts (20 μg protein per lane) isolated from upper non-infected leaves at 2, 4 and 8 days after bacteria inoculation were analyzed by Western blotting. The experiment was performed twice, with similar results.

were dead (Figure 6b), indicating that cells associated with the vascular tissue were dying at the same time as the mesophyll cells. In contrast, in leaves infected with the avirulent pathovar, many living cells were still present in the vascular bundle (Figure 6d) at a time (12 hpi) when most other cells had completely disintegrated (see also Figure S1).

Discussion

Plant resistance is often accompanied by rapid tissue necrotization at pathogen entry sites, referred to as HR. This PCD-related process is genetically controlled (Greenberg and Yao, 2004 and references therein). While PCD in plants has been classified into various categories, such as apoptosis, programmed oncosis, non-lysosomal cell death and autophagy, all these mechanisms of cell death execution have been suggested to operate during the HR (van Doorn and Woltering, 2005; Jones, 2000; Levine *et al.*, 1996; Liu *et al.*, 2005). However, it has also been observed that the characteristic features associated with HR can be dependent on the pathogen involved. Cowpea cells undergoing HR in response to either host or non-host biotrophic fungi varied in the timing and pattern of cellular changes that occurred after cessation of cytoplasmic streaming (Christopher-Kozjan and Heath, 2003). These differences included the position of the nucleus relative to the invading fungus, maintenance of cytoplasmic transvacuolar strands, and the presence of Brownian-like motion within the cytoplasm. In addition, application of synthetic caspase inhibitors and RGD-motif peptides were found to influence host and non-host HRs in different ways. These data were interpreted to indicate that two distinct morphotypes of cell death were being elicited by host and non-host biotrophic fungi (Christopher-Kozjan and Heath, 2003).

Figure 6. Differences in degradation of cells surrounding conductive elements after treatment with two pathovars of *Pseudomonas syringae*.
Leaves infiltrated with Psm (a, b) at 3 and 4.5 hpi, respectively; and Pst (c, d) at 6 and 12 hpi, respectively. After fixation and embedding, material was subjected to TEM analysis. Bars, 5 μm. De, dead cell; Se, sieve element; X, xylem. The experiment was performed twice, for details see Experimental procedures.

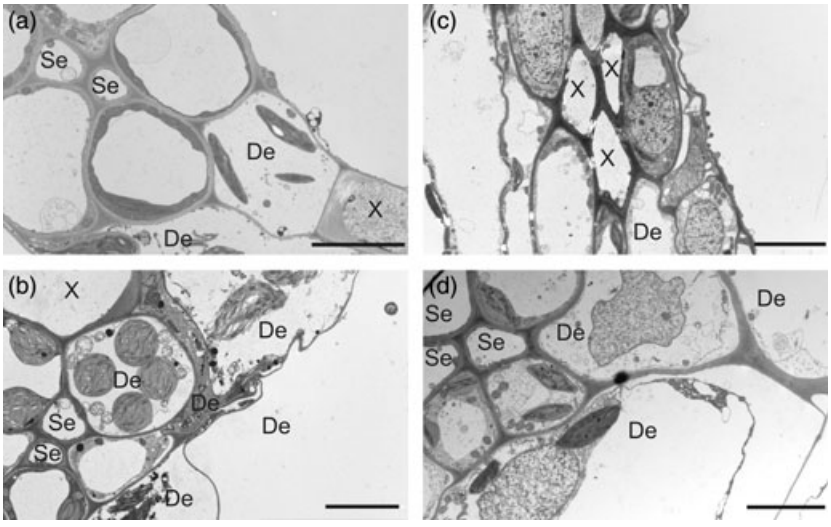

In the present study, we have examined the HRs elicited in tobacco by two pathovars of *P. syringae*, pv. *tabaci* and pv. *maculicola*, that trigger host- and non-host resistance, respectively. It was previously reported by Klement (1963) that tissue decay in tobacco infiltrated with an avirulent pathogen progressed more slowly than that associated with non-host pathogen infection, a pattern that is fully confirmed by our results. The simultaneous occurrence of macroscopic HR, massive ion leakage and Evans blue uptake suggests that symptom development in response to Psm is initiated by irreversible membrane rupture. In contrast, after Pst inoculation there was a distinct time lapse (approximately 3 h) between the first signs of tissue collapse and the appearance of indicators of plasma membrane discontinuity. Although many cells in the TEM sections showed breaks in tonoplast and/or plasma membrane (data not shown), this approach does not allow us to establish unambiguously a precise sequence of membrane-damage events. However, the sparse deposition of callose after Psm infiltration could reflect a rapid and irreversible loss of membrane function (Figure S2e,f). In contrast, abundant callose deposits formed following infection with Pst (Figure S2h,i).

Detailed ultrastructural analysis of dying cells in bacteria-infiltrated tissues revealed that, as expected, cytological alterations distinctly preceded macroscopic necrotization. The two pathosystems differed, however, in the order in which changes in organelle morphology occurred. Following Psm inoculation (Figure 2a), chloroplasts rapidly assumed abnormal shapes, and by 4.5 hpi they had disintegrated. Despite the destruction of this cellular compartment, only minor changes were observed in transparency of the nucleoplasm, and even at relatively late stages the nuclear envelope remained intact (see also Figure S1h). Consistent with this, DAPI staining did not reveal any marked abnormalities in nucleus structure (Figure 2b). In contrast, the nuclei in Pst-inoculated zones underwent dynamic changes, as indicated by TEM and fluorescence microscopy, and Pst-evoked cell death culminated in breakdown of the chloroplasts and mitochondria (Figure S1p).

Finally, the ability of synthetic caspase inhibitors to abolish tissue collapse triggered by Pst, but not that elicited by Psm, emphasizes the distinctness of the processes underlying these two interactions. Interestingly, although VPEs have been identified as targets of these synthetic caspase inhibitors in plants (Hatsugai *et al.*, 2004; Nakaune *et al.*, 2005; Rojo *et al.*, 2004), we did not detect any increased accumulation of VPE transcripts in either pathosystem by 12 hpi, a time by which symptoms had fully developed in both interactions (data not shown). In contrast, the expression of *Hsr203J* and *Hin1*, genes commonly used as molecular markers of HR-related cell death (Gopalan *et al.*,1996; Pontier *et al.*, 1994), was induced early in response to bacterial infection (Figure 1g). Although the level of expression was much higher in response to Pst infection, the temporal pattern of mRNA accumulation was similar for each gene. Our results suggest that although, as shown previously, *Hsr203J* and *Hin1* are good markers of HR, they are not suitable to discriminate between different types of cell death triggered by bacteria.

Non-host resistance as manifested by PCD in the infected tissue seems to be a primary defense response, but some bacteria manage to overcome it through acquisition of virulence factors that allow them to colonize plants. It was has been suggested that suppression of plant PCD may be one strategy employed by the bacterial pathogen to ensure survival in host plants (Kang *et al.*, 2004). Several effectors of the type III secretion system that suppress PCD have been identified (Abramovitch and Martin, 2004; Abramovitch *et al.*, 2003; Espinosa *et al.*, 2003; Jamir *et al.*, 2004; Kang *et al.*, 2004; Nomura *et al.*, 2005) and, interestingly, they differ in specificity. For example, AvrPto suppresses only cell death caused by certain non-host pathogens (Kang *et al.*, 2004), a pattern that supports the idea that distinct pathways can underlie PCD in host and non-host resistance. However, the fact that caspase inhibitors can affect some host HRs (our studies) and some non-host HRs (Christopher-Kozjan and Heath, 2003; del Pozo and Lam, 1998) suggests that the ability of a pathogen to colonize the plant may not be a reliable criterion to be used in cell death classification, as the morphotype of cell death triggered in the infected plant is likely to reflect the specific evolutionary history of the given plant–pathogen combination.

The importance of the HR in limiting pathogen growth is still being debated, but this uncertainty may reflect different degrees of HR contribution to resistance, depending on the specific plant–pathogen interaction (Greenberg and Yao, 2004 and references therein). It is interesting that, as shown in Figure S3, the HR evoked by both Psm and Pst did not appear to lead to destruction of the invading bacteria, suggesting that other, indirect mechanisms, such as physical trapping in necrotized tissues, may be involved in the arrest of bacterial colonization.

A typical set of defense responses was induced locally in Psm-infiltrated tobacco leaves, including acquired resistance (Figures 3 and 4). Surprisingly, no LDAR was established in non-infiltrated leaves of Psm-pre-treated plants. Moreover, we failed to detect biochemical (SA induction, data not shown) or molecular (PR-1a induction, Figure 5b) markers of LDAR in upper leaves. In contrast, plants pre-inoculated with Pst exhibited enhanced resistance to secondary infection in both local and systemic leaves (Figures 4 and 5).

Thus tobacco inoculated with Psm could be regarded as a system where local acquired resistance is uncoupled from development of LDAR, presumably because of some perturbation in long-distance signaling. In this respect, establishment of acquired resistance is analogous to virus spreading throughout a plant, where two distinct processes,

short- and long-distance movement of virus particles, can be distinguished, and the non-vascular/vascular tissue interface represents a major barrier to long-distance movement (Leisner and Howell, 1993). As this interface might also be critical for mobile signaling during LDAR, we examined the anatomy of the vascular bundles in tobacco leaves infected with the two bacterial pathovars. In contrast to Psm-infiltrated leaves, most bundle sheath cells in Pst-infiltrated leaves remained alive after death of surrounding mesophyll cells (Figure 6b,d). These data strongly suggest that the success of long-distance signaling, and thus LDAR induction, can be determined by the state of vascular bundles at the time the mobile signal is generated and transmitted.

Other scenarios are also possible, however, including models in which there are two types of signal molecule for short- and long-distance transmission and/or different carriers, and in which only one type of signal molecule and/or carrier is generated in the Psm system. While it is also possible that Psm manipulates or directly inhibits the systemic signal generated by tobacco (Cui *et al.*, 2005), we found that infiltrating Psm into tobacco leaves in the midst of the Pst-induced signal transmission failed to interfere with the development of LDAR (data not shown). We therefore tend to favor the hypothesis that the lack of LDAR in Psm-pre-treated tobacco plants is related primarily to rapid collapse of the bundle sheath cells. Further experiments are necessary to establish whether the timing of vascular tissue degradation depends on the type of PCD initiated by infection, and whether rapid blocking of vascular transmission is ultimately to the benefit of host plants or pathogens.

Experimental procedures

Plant material and growth conditions

Tobacco plants (*Nicotiana tabacum* cv. Xanthi-nc) were grown for 6 weeks in soil under controlled environmental conditions (22°C, 16 h light, 8 h dark) as described previously (Talarczyk *et al.*, 2003).

Bacterial strains and infection

Pseudomonas syringae pv. *maculicola* M2 and *P. syringae* pv. *tabaci* strains (a kind gift of Dr Mathias Ullrich) were maintained on nutrient agar and stored at 18°C. Bacteria for inoculation were cultured overnight (18 h) on King's B medium at 28°C with vigorous shaking, and centrifuged at 3500 ***g*** for 10 min. The bacterial pellet was washed once and resuspended in sterile miliQ water, and adjusted to 10^8 cfu ml^{-1}. Three fully expanded leaves of tobacco were inoculated with bacteria or water using a needle-less hypodermic syringe. For macroscopic observation, conductivity assay, Evans blue staining, SA and O_2^- measurements, the leaves were completely infiltrated with bacteria. For other experiments, bacteria were applied patchwise. At selected time points, leaf discs were cut from infiltrated zones or whole leaves were harvested and, after mid-rib excision, stored at –80°C for further analysis.

Assessment of acquired resistance

Appropriate leaves of pre-inoculated tobacco plants were dusted with carborundum and rubbed with TMV strain U1 suspension (1 μg ml^{-1}), and after 15 min were rinsed with tap water. The diameters of necrotic lesions were measured 7 days post-infection.

Caspase inhibitors

Tobacco leaves were co-infiltrated with bacteria and one of two synthetic caspase inhibitors, the chloromethylketone Ac-YVAD-CMK or the aldehyde Ac-DEVD-CHO (Alexis Corp., Lausen, Switzerland, http://www.alexis-biochemicals.com). The inhibitors were pre-dissolved in DMSO and diluted with water to 200 μM final concentration in 0.4% v/v DMSO. Aqueous DMSO (0.4% v/v) was used as a negative control.

RNA analysis

Total RNA was isolated from leaves as described previously (Linthorst *et al.*, 1993). For Northern blot analyses, 10 μg RNA was separated on a 1% agarose gel in 15 mM sodium phosphate buffer (pH 6.5), and transferred to Hybond N membranes (Amersham Biosciences, http://www6.amershambiosciences.com). Hybridization was performed at 65°C in 250 mM sodium phosphate buffer (pH 7.0), 1 mM EDTA, 7% (w/v) SDS and 1% (w/v) BSA with one of the following randomly labeled probes: (i) 592 bp *Hsr203J* cDNA (Pontier *et al.*, 1994); (ii) 871 bp *Hin1* cDNA; (iii) 900 bp acidic *PR-1a* cDNA (Cutt *et al.*, 1988); (iv) 790 bp basic *PR-1b* cDNA (Brederode *et al.*, 1991); (v) 800 bp acidic *PR-5a* (Brederode *et al.*, 1991); (vi) 700 bp basic *PR-5b* cDNA (Brederode *et al.*, 1991); (vii) 1550 bp *18S rDNA*.

Protein analysis

Proteins were extracted in buffer containing 50 mM Tris pH 8.0, 1 mM EDTA, 12 mM β-mercaptoethanol and 10 μg ml^{-1} phenylmethylsulfonyl fluoride (PMSF). Protein content was measured by the Bradford method using a commercially available reagent (BioRad Laboratories, http://www.bio-rad.com). Extracts were fractionated on 12.5% SDS-PAGE and subjected to immunoblot analysis using a specific mouse anti-PR-1 monoclonal antibody (a gift from Professor D.F. Klessig) and alkaline phosphatase-conjugated anti-mouse antibodies from Sigma-Aldrich (http://www.sigmaaldrich.com). Immunoblots were developed using the NBT/BCIP (5-bromo-4-chloro-3-indolyl phosphate, toluidine salt) colorimetric detection kit from Roche Applied Science (http://www.roche.com).

Quantification and characterization of SA and SAG

Free SA was extracted and quantified essentially as described by Raskin *et al.* (1989) with modifications introduced by Malamy *et al.* (1992). HPLC was performed as described previously (Malamy *et al.*, 1990). The salicylic acid β-glucoside (SAG) was quantified as described by Malamy *et al.* (1992). Total SA was calculated as a sum of free SA and SAG.

Ion-leakage assay

At given time points, eight leaf discs (1 cm diameter) were cut from infiltrated zones and floated abaxial side up on 5 ml miliQ water for 10 min at 18°C with gyratory agitation (50 rpm). The conductivity of

the water was subsequently measured with a CDM83 conductivity meter (Radiometer Copenhagen, http://www.radiometer.com) and expressed in $\mu S\ cm^{-1}$.

O_2^- detection

Superoxide anion concentrations were assayed spectrophotometrically (Doke, 1983) by monitoring the reduction of NBT (Sigma-Aldrich) at 580 nm after incubation with eight leaf discs cut from appropriate plants. Inoculations were performed on two plants for each experiment.

Membrane integrity test

Membrane integrity was tested according to Yamamoto *et al.* (2001) with modifications. Four leaf discs were stained with aqueous Evans blue (2% w/v) for 10 min at 18°C, 50 r.p.m. Afterwards the leaf discs were rinsed briefly with miliQ water and cleared with boiling ethanol (96%) to remove the chlorophyll.

Tissue preparation and morphological analysis of nuclei

Leaf pieces from Psm-, Pst- or mock-inoculated plants were fixed in 4% (w/v) methanol-free paraformaldehyde solutions in PBS (pH 7.4) overnight at 4°C, washed and dehydrated. The fixed samples were embedded in Paraplast Plus (Sherwood Medical Co., St Louis, MO, USA, http://www.sigmaaldrich.com), and sections (10 μm) were mounted on poly-L-lysine-coated slides, deparaffinized with xylene and rehydrated through a graded ethanol series. To study nuclear morphology, tissues were stained with aqueous 4′,6′-diamidino-2-phenylindole (DAPI, 1 $\mu g\ ml^{-1}$, Sigma-Aldrich), and nuclei were examined under the fluorescence microscope (UV, excitation wavelength λ = 360 nm).

TEM analysis

For light and TEM analyses, fragments of leaves were dissected from mock-, Psm- or Pst-inoculated tobacco plants. Samples were collected at 1.5, 3.0, 4.5 and 6.0 hpi for Psm-inoculated plants, and at 3.0, 6.0, 9.0, 12.0 and 13.5 hpi for Pst-inoculated plants, from two independent inoculations (three samples for each treatment were analyzed). The sites where syringes had been applied to the leaves were carefully avoided. Samples were fixed in a mixture of 4% (w/v) paraformaldehyde and 2% (v/v) glutaraldehyde in 0.05 M sodium cacodylate buffer (pH 7.2) for 2 h at room temperature. They were then washed, post-fixed with osmium tetroxide, dehydrated, infiltrated with Fluka Epon epoxy resin (http://www.sigmaaldrich.com) and polymerized according to the procedure of Golinowski *et al.* (1996). Semi-thin (2.0 μm thick) sections were made with a Leica (http://www.leicamicrosystems.com) RM2165 rotary microtome, attached to glass slides, and stained with hot (60°C) aqueous Crystal Violet (1%, w/v) for 30 sec, followed by abundant washing. After air-drying, the sections were inspected under an Olympus AX70 Provis light microscope and images were captured with an Olympus DP50 digital camera (http://www.olympus-global.com/). Ultra-thin (60–90 nm thick) sections were made with a Leica UCT ultramicrotome and, after mounting on formvar-coated copper single-slot grids, stained with uranyl acetate and lead citrate for 15 and 5 min, respectively. Stained sections were examined in an FEI (http://www.fei.com) M268D Morgagni TEM equipped with an SIS (http://www.soft-imaging.net) Morada digital camera running under SIS ITEM software. Images collected from both microscopes were adjusted for similar brightness and contrast, and resized using Adobe PHOTOSHOP 7 software.

Callose staining

To visualize callose deposition, leaf discs were cut from inoculated plants and stained with 0.01% (w/v) aniline blue as described elsewhere (Gómez-Gómez *et al.*, 1999). The stained discs mounted in 70% glycerol, 30% staining solution were examined using ultraviolet epifluorescence (Nikon Eclipse E800, DAPI filter (http://www.nikon-instruments.jp)).

Statistical analysis

Data are reported as the mean ± SD. The results were compared statistically using a two-tailed Student's *t*-test, and differences were considered significant if P values were <0.05 or as indicated in the legends.

Upon request, all novel materials described here will be made available in a timely manner for non-commercial research purposes.

Acknowledgements

This work was partially supported by a grant (No. PBZ-KBN-110/P04/2004/18) from the Polish Ministry of Science and Higher Education. We thank Enno Krebbers for critical reading of the manuscript. The ultramicrotomy work of Malgorzata Wasilewska-Gomulka and Ewa Znojek is gratefully acknowledged.

Supplementary Material

The following supplementary material is available for this article online:

Figure S1. Images showing anatomical and ultrastructural changes in leaves infected with two pathovars of *Pseudomonas syringae.* Samples were collected from zones infiltrated with Psm at 1.5 (c, d), 4.5 (e, f) and 6 hpi (g, h); and Pst at 3 (k, l), 9 (m, n) and 12 hpi (o, p). Left-hand figures show sections stained with crystal violet and observed by light microscopy; right-hand figures show corresponding TEM micrographs. (a, b, i, j) Sections of control non-inoculated leaves. Ch, chloroplast; M, mitochondrion; Nu, nucleus; VB, vascular bundle; De, dead cell. Bars, 25 and 2 μm for left and right panels, respectively.

Figure S2. Callose deposition in leaves inoculated with two different strains of *Pseudomonas syringae*. Tissue from bacteria-infiltrated zones was subjected to light and fluorescence microscopy after aniline blue staining (a, b, d, e, g, h). Bars, 150 μm. The same material was subjected to TEM studies. Arrowheads indicate callose depositions adjacent to bacteria infection sites; asterisks, bacteria cells. Bars, 2 μm. (a–c) mock-; (d–f) Psm-; (g–i) Pst-inoculated leaves at 9, 4.5 and 9 hpi, respectively.

Figure S3. Presence of live bacteria in collapsed tissue. Sections were prepared from Psm-inoculated (a, b) or Pst-inoculated leaves (c, d) at 6 and 13.5 hpi, respectively. Left panel, sections stained with crystal violet and observed by light microscopy; right panel, images analyzed by TEM. Arrowhead, dividing bacterial cells. Bars, 25 μ (a, c) and 2 μm (b, d).

This material is available as part of the online article from http://www.blackwell-synergy.com

References

Abramovitch, R.B. and Martin, G.B. (2004) Strategies used by bacterial pathogens to suppress plant defenses. *Curr. Opin. Plant Biol.* **7**, 356–364.

Abramovitch, R., Kim, Y.-J., Chen, S., Dickman, M.B. and Martin, G.B. (2003) *Pseudomonas* type III effector AvrPtoB induces plant disease susceptibility by inhibition of host programmed cell death. *EMBO J.* **22**, 60–69.

van der Biezen, E.A. and Jones, J.D. (1998) Plant disease-resistance proteins and the gene-for-gene concept. *Trends Biochem. Sci.* **23**, 454–456.

Boller, T. (2005) Peptide signalling in plant development and self/non-self perception. *Curr. Opin. Cell Biol.* **17**, 116–122.

Brederode, F.T., Linthorst, H.J. and Bol, J.F. (1991) Differential induction of acquired resistance and PR gene expression in tobacco by virus infection, ethephon treatment, UV light and wounding. *Plant Mol. Biol.* **17**, 1117–1125.

Christopher-Kozjan, R. and Heath, M.C. (2003) Cytological and pharmacological evidence that biotrophic fungi trigger different cell death execution processes in host and nonhost cells during the hypersensitive response. *Physiol. Mol. Plant Pathol.* **62**, 265–275.

Cui, J., Bahrami, A.K., Pringle, E.G., Hernandez-Guzman, G., Bender, C.L., Pierce, N.E. and Ausubel, F.M. (2005) *Pseudomonas syringae* manipulates systemic plant defenses against pathogens and herbivores. *Proc. Natl Acad. Sci. USA*, **102**, 1791–1796.

Cutt, J.R., Dixon, D.C., Carr, J.P. and Klessig, D.F. (1988) Isolation and nucleotide sequence of cDNA clones for the pathogenesis-related proteins PR1a, PR1b and PR1c of *Nicotiana tabacum* cv. Xanthi-nc induced by TMV infection. *Nucl. Acids Res.* **16**, 9861.

Doke, N. (1983) Involvement of superoxide anion generation in the hypersensitive response of potato tuber tissues to infection with an incompatible race of *Phytophtora infestans* and to the hyphal wall components. *Physiol. Plant Pathol.* **23**, 345–357.

van Doorn, W.G. and Woltering, E.J. (2005) Many ways to exit? Cell death categories in plants. *Trends Plant Sci.* **10**, 117–122.

Espinosa, A., Guo, M., Tam, V.C., Qing Fu, Z. and Alfano, J.R. (2003) The *Pseudomonas syringae* type III-secreted protein HopPtoD2 possesses protein tyrosine phosphatase activity and suppresses programmed cell death in plants. *Mol. Microbiol.* **49**, 377–387.

Golinowski, W., Grundler, F.M.W. and Sobczak, M. (1996) Changes in the structure of *Arabidopsis thaliana* during female development of the plant-parasitic nematode *Heterodera schachtii*. *Protoplasma*, **194**, 103–116.

Gómez-Gómez, L., Felix, G. and Boller, T. (1999) A single locus determines sensitivity to bacterial flagellin in *Arabidopsis thaliana*. *Plant J.* **18**, 277–284.

Gopalan, S., Wei, W. and He, S.Y. (1996) *hrp* gene-dependent induction of *hin1*: a plant gene activated rapidly by both harpins and the avrPto gene-mediated signal. *Plant J.* **10**, 591–600.

Greenberg, J.T. and Yao, N. (2004) The role and regulation of programmed cell death in plant–pathogen interactions. *Cell. Microbiol.* **6**, 201–211.

Hara-Nishimura, I., Hatsugai, N., Nakaune, S., Kuroyanagi, M. and Nishimura, M. (2005) Vacuolar processing enzyme: an executor of plant cell death. *Curr. Opin. Plant Biol.* **8**, 404–408.

Hatsugai, N., Kuroyanagi, M., Yamada, K., Meshi, T., Tsuda, S., Kondo, M., Nishimura, M. and Hara-Nishimura, I. (2004) A plant vacuolar protease, VPE, mediates virus-induced hypersensitive cell death. *Science*, **305**, 855–858.

Heath, M.C. (1998) Apoptosis, programmed cell death and the hypersensitive response. *Eur. J. Plant Pathol.* **104**, 117–124.

Heath, M.C. (2000a) Nonhost resistance and nonspecific plant defenses. *Curr. Opin. Plant Biol.* **3**, 315–319.

Heath, M.C. (2000b) Hypersensitive response-related death. *Plant Mol. Biol.* **44**, 321–334.

Innes, R.W. (2004) Guarding the goods. New insights into the central alarm system of plants. *Plant Physiol.* **135**, 695–701.

Jamir, Y., Guo, M., Oh, H.-S., Petnicki-Ocwieja, T., Chen, S., Tang, X., Dickman, M.B., Collmer, A. and Alfano, J.R. (2004) Identification of *Pseudomonas syringae* type III effectors that can suppress programmed cell death in plants and yeast. *Plant J.* **37**, 554–565.

Jones, A. (2000) Does the plant mitochondrion integrate cellular stress and regulate programmed cell death? *Trends Plant Sci.* **5**, 225–230.

Kang, L., Tang, X. and Mysore, K.S. (2004) *Pseudomonas* type III effector AvrPto suppresses the programmed cell death induced by two nonhost pathogens in *Nicotiana benthamiana* and tomato. *Mol. Plant Microbe Interact.* **17**, 1328–1336.

Katagiri, F., Thilmony, R. and He, S.Y. (2002) The *Arabidopsis thaliana–Pseudomonas syringae* interaction. In *Arabidopsis Book* (Somerville, C.R. and Meyerowitz, E.M., eds). Rockville, MD, USA: American Society of Plant Biologists, pp. 1–35.

Klement, Z. (1963) Rapid detection of the pathogenicity of phytopathogenic pseudomonads. *Nature*, **199**, 299–300.

Leisner, S.M. and Howell, S.H. (1993) Long-distance movement of viruses in plants. *Trends Microbiol.* **1**, 314–317.

Levine, A., Pennell, R.I., Alvarez, M.E., Palmer, R. and Lamb, C. (1996) Calcium-mediated apoptosis in plant hypersensitive disease resistance response. *Curr. Biol.* **6**, 427–437.

Linthorst, H.J., Van der Does, C., Brederode, F.T. and Bol, J.F. (1993) Circadian expression and induction by wounding of tobacco genes for cysteine proteinase. *Plant Mol. Biol.* **21**, 685.

Liu, Y., Schiff, M., Czymmek, K., Talloczy, Z., Levine, B. and Dinesh-Kumar, S.P. (2005) Autophagy regulates programmed cell death during the plant innate immune response. *Cell*, **121**, 567–577.

Malamy, J., Carr, J.P., Klessig, D.F. and Raskin, I. (1990) Salicylic acid – a likely endogenous signal in the resistance response of tobacco to tobacco mosaic virus infection. *Science*, **250**, 1002–1004.

Malamy, J., Hennig, J. and Klessig, D.F. (1992) Temperature-dependent induction of salicylic acid and its conjugates during the resistance response to tobacco mosaic virus infection. *Plant Cell*, **4**, 359–366.

Nakaune, S., Yamada, K., Kondo, M., Kato, T., Tabata, S., Nishimura, M. and Hara-Nishimura, I. (2005) A vacuolar processing enzyme, δVPE, is involved in seed coat formation at the early stage of seed development. *Plant Cell*, **17**, 876–887.

Nimchuk, Z., Eulgem, T., Holt, B.F., III and Dangl, J.L. (2003) Recognition and response in the plant immune system. *Annu. Rev. Genet.* **37**, 579–609.

Nomura, K., Melotto, M. and He, S.-Y. (2005) Suppression of host defense in compatible plant–*Pseudomonas* interactions. *Curr. Opin. Plant Biol.* **8**, 361–368.

Nürnberger, T. and Lipka, V. (2005) Non-host resistance in plants: new insights into an old phenomenon. *Mol. Plant Pathol.* **6**, 335–345.

Pontier, D., Godiard, L., Marco, Y. and Roby, D. (1994) *hsr203 J*, a tobacco gene whose activation is rapid, highly localized and specific for incompatible plant/pathogen interactions. *Plant J.* **5**, 507–521.

del Pozo, O. and Lam, E. (1998) Caspases and programmed cell death in the hypersensitive response of plants to pathogens. *Curr. Biol.* **8**, 1129–1132.

Raskin, I., Turner, I.M. and Melander, W.R. (1989) Regulation of heat production in the inflorescences of an *Arum* lily by endogenous salicylic acid. *Proc. Natl Acad. Sci. USA*, **86**, 2214–2218.

Rojo, E., Martin, R., Carter, C. *et al.* (2004) VPEγ exhibits a caspase-like activity that contributes to defense against pathogens. *Curr. Biol.* **14**, 1897–1906.

Sanmartin, M., Jaroszewski, L., Raikhel, N.V. and Rojo, E. (2005) Caspases. Regulating death since the origin of life. *Plant Physiol.* **137**, 841–847.

Sarkar, S.F. and Guttman, D.S. (2004) Evolution of the core genome of *Pseudomonas syringae*, a highly clonal endemic plant pathogen. *Appl. Environ. Microbiol.* **70**, 1999–2012.

Sawada, H., Suzuki, F., Matsuda, I. and Saitou, N. (1999) Phylogenetic analysis of *Pseudomonas syringae* pathovars suggests the horizontal gene transfer of *argK* and the evolutionary stability of *hrp* gene cluster. *J. Mol. Evol.* **49**, 627–644.

Talarczyk, A., Krzymowska, M., Borucki, W. and Hennig, J. (2003) Effect of *Saccharomyces cerevisiae CTA1* gene expression on response of tobacco plants to Tobacco Mosaic Virus infection. *Plant Physiol.* **129**, 1032–1044.

Tronchet, M., Ranty, B., Marco, Y. and Roby, D. (2001) HSR203 antisense suppression in tobacco accelerates development of hypersensitive cell death. *Plant J.* **27**, 115–127.

Yamamoto, Y., Kobayashi, Y. and Matsumoto, H. (2001) Lipid peroxidation is an early symptom triggered by aluminium, but not the primary cause of elongation inhibition in pea roots. *Plant Physiol.* **125**, 199–208.

